
Gaze Beyond the Frame: Forecasting Egocentric 3D Visual Span

Heeseung Yun¹, Joonil Na¹, Jaeyeon Kim², Calvin Murdock³, Gunhee Kim¹
¹Seoul National University, ²Carnegie Mellon University, ³Reality Labs Research at Meta
<https://hs-yn.github.io/GazeBeyondFrame/>

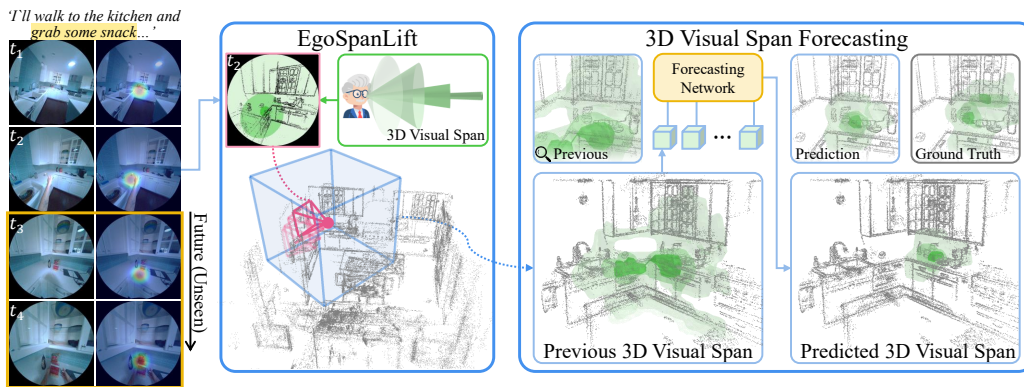


Figure 1: *Can we forecast our gaze beyond the frame?* We aim to predict a person’s future visual focus in 3D surrounding environment by lifting egocentric 2D gaze history to 3D regions and forecasting future 3D visual spans from previous observations.

Abstract

People continuously perceive and interact with their surroundings based on underlying intentions that drive their exploration and behaviors. While research in egocentric user and scene understanding has focused primarily on motion and contact-based interaction, forecasting human visual perception itself remains less explored despite its fundamental role in guiding human actions and its implications for AR/VR and assistive technologies. We address the challenge of egocentric 3D visual span forecasting, predicting where a person’s visual perception will focus next within their three-dimensional environment. To this end, we propose EgoSpanLift, a novel method that transforms egocentric visual span forecasting from 2D image planes to 3D scenes. EgoSpanLift converts SLAM-derived keypoints into gaze-compatible geometry and extracts volumetric visual span regions. We further combine EgoSpanLift with 3D U-Net and unidirectional transformers, enabling spatio-temporal fusion to efficiently predict future visual span in the 3D grid. In addition, we curate a comprehensive benchmark from raw egocentric multisensory data, creating a testbed with 364.6K samples for 3D visual span forecasting. Our approach outperforms competitive baselines for egocentric 2D gaze anticipation and 3D localization while achieving comparable results even when projected back onto 2D image planes without additional 2D-specific training.

1 Introduction

People continuously perceive and interact with their surrounding environments in everyday life. Underlying these interactions are their intentions, which drive them to actively explore their surround-

ings and engage in various behaviors. Understanding how individuals will perceive contexts and take actions in advance becomes a crucial element in comprehending their overall behavior patterns. The ability to accurately anticipate behavior not only reduces latency in real-time egocentric applications but also serves as a foundation for proactively delivering information and services in our daily lives, *e.g.*, immersive VR/AR, ambient computing, and assisting individuals with impairments.

To better understand a person’s intentions, research in egocentric user and scene understanding has been widely explored, primarily involving action and contact-based interaction. For instance, when given egocentric visual or multimodal context, studies have focused on predicting subsequent human actions [1, 2, 3] or localizing regions in 2D images where interaction will occur [4]. Recent studies have actively investigated human pose or motion forecasting in 3D space [5, 6, 7], as well as contact location prediction during object interactions [8, 9]. However, attempts to forecast human visual perception itself remain less explored. Studies in vision science and cognitive psychology suggest that perceptual exploration significantly influences human motion [10, 11, 12, 13], and intuitively, most of our daily interactions follow perception, *i.e.*, we look before we leap. Therefore, forecasting visual perception is essential for proactively understanding and anticipating human behavior.

In this work, we address the novel challenge of *egocentric 3D visual span forecasting*—forecasting where a person’s visual perception will be focused in the surrounding environment. We draw inspiration from the vision science literature regarding text reading [14, 15] and object/scene perception [16, 17, 18], where the visual span often refers to the fixated region of human vision from peripheral awareness to precise foveal gaze fixations. In our context, we adopt this term as *3D Visual Span* to refer to egocentric visual focus in 3D surroundings for addressing daily and casual behaviors and interactions. While previous research has shown impressive results in predicting egocentric future gaze fixations on 2D image frames [19, 20], forecasting gaze for dynamic scenarios in 2D remains unclear. Gaze anticipation requires jointly modeling the user’s self-motion and attention—both of which are naturally directed toward specific locations in 3D space rather than arbitrary regions in 2D projections. That is, modeling visual span as 3D regions offers a more accurate and consistent representation of perceptual focus even beyond our current observations, unlocking promising egocentric applications that call for robust and proactive content rendering [21, 22].

Our main contribution comprises three key components: (i) a method for bridging egocentric visual spans and 3D scenes, (ii) a framework for forecasting future spans, and (iii) a newly curated benchmark from raw egocentric multisensory data. First, we propose *EgoSpanLift*, a novel method that lifts visual spans in 2D image frames into structured 3D volumetric regions, as illustrated in Fig. 1. Unlike existing 3D egocentric localization approaches on motion trajectories or object interactions, our method uniquely transforms SLAM-derived keypoints into gaze-compatible geometry to precisely extract volumetric regions corresponding to 3D visual span. *EgoSpanLift* encodes multi-level span information grounded in vision science [15]—ranging from wide head-orientation-based regions to fine-grained foveal fixations—enabling a semantically rich understanding of where and how people look in space. Building on this, we introduce an autoregressive forecasting framework that combines *EgoSpanLift* with a 3D U-Net for spatial representation using a unidirectional transformer for temporal modeling, effectively capturing the evolving dynamics of egocentric visual attention.

To establish a testbed at scale, we rigorously curate raw egocentric multisensory data streams [23, 24] for benchmarking 3D visual span forecasting under daily and skilled activity scenarios, namely FoVS-Aria and FoVS-EgoExo, covering a total of 364.6K samples. Our framework outperforms several competitive baselines, including frameworks for 3D egocentric localization and 2D gaze prediction models equipped with our *EgoSpanLift*. We conduct extensive analysis across varying spatio-temporal windows and activity categories. Notably, when our 3D visual span predictions are back-projected onto 2D image planes, they achieve accuracy on par with 2D-specific models even without 2D-specific training, demonstrating the versatility and robustness of modeling gaze in 3D.

2 Related Work

Egocentric Anticipation of User Behavior. Predicting user behavior from egocentric observations represents one of the core challenges in egocentric user and scene understanding. The EPIC-Kitchens dataset [1] introduced the challenge of predicting future action classes within procedural kitchen activities. Various approaches have been proposed to address this problem, including dual LSTM architectures for past and future modeling [2], and contrastive learning with RNNs for future visual

feature learning [3]. Beyond semantic action classification, studies have also proposed methods for predicting locomotion trajectories from current user observations [4, 25, 26]. For more detailed user posture prediction beyond trajectories [27], recent work has utilized reinforcement learning-based recurrent control [5], MLP-based residual modeling [6], and video-pose bimodal transformers [7].

Egocentric Gaze Prediction Understanding and predicting human gaze behavior is crucial for modeling various aspects of perception and interaction. Many studies primarily aim to estimate gaze direction from facial/head images [28, 29, 30], predict the object of visual attention [31, 32, 33, 34, 35], focus on VR/mobile scenarios [36, 37, 38, 39, 40], and model the interplay with language [41, 42]. Estimating and predicting gaze from egocentric perspectives pose additional challenges due to complex egocentric scenes and a combination of dynamic gaze shifts with frequent head and body movements, *i.e.*, self-motion. Egocentric gaze estimation often involves bottom-up saliency [43], joint gaze-action prediction [44], and global-local correlation [45].

On the other hand, the frontier of gaze anticipation remains relatively unexplored due to insufficient input context for predicting *future* frames. Zhang *et al.* [19] employ a GAN to synthesize future frames and forecast gaze locations, while Lai *et al.* [20] also introduce a multimodal anticipation model that uses contrastive spatial/temporal separable fusion to capture audio-visual correlations and improve future gaze prediction. However, predicting gaze in 2D images is often ill-posed in dynamic scenarios, as it requires jointly modeling the user’s self-motion and attention, which are inherently directed toward specific locations in 3D rather than arbitrary regions in 2D frames. In this work, we address these issues by directly predicting the user’s gaze and visual focus in 3D scenes through spatio-temporal fusion of volumetric representations.

Egocentric 3D Interaction. Research on egocentric interaction has evolved from 2D to 3D understanding and from contact-based to intention-based analysis. Earlier work on 2D image interaction analysis primarily addresses hand detection, segmentation, and pose estimation [46, 47, 48, 49, 50]. Moving beyond 2D approaches, 3D-based frameworks leverage hand poses and object interactions involving physical contacts from RGB(-D) inputs [51, 52, 53, 54, 55, 56, 57], allowing for precise prediction of hand trajectories and action targets [58, 59, 60]. Recent line of work interprets potential 3D interaction regions as spatial affordances, learned from either synthesized geometry and motion [9] or intentional cues in 2D interaction images [8].

Concurrent research with ours, FICTION [61], focuses on 4D human-object interaction. FICTION jointly predicts the 3D bounding box of objects involved in physical interactions along with the user’s spatial location and body poses where contact occurs at future time steps. A key distinction of our work is that it address the forecasting problem for 3D regions where the user’s visual perception is focused and precedes these everyday actions and interactions. Our predictions take the form of multi-level 3D volumetric regions of the visual span, enabling more fine-grained forecasting of potential interaction hotspots than bounding boxes.

3 EgoSpanLift: Lifting Egocentric Gaze Prediction from 2D to 3D

3.1 Preliminary: Simultaneous Localization and Mapping

Simultaneous Localization and Mapping (SLAM) refers to the problem of jointly estimating an agent’s position and reconstructing the surrounding 3D environment from sequential observations. It is often formulated as a probabilistic framework that maximizes the posterior distribution $P(\mathbf{x}_t, \mathbf{m} \mid \mathbf{c}_{1..t-1}, \mathbf{o}_{1..t-1})$, where \mathbf{x}_t denotes the pose at time t , \mathbf{m} is the 3D mapping information, and $\mathbf{c}_{1..t-1}, \mathbf{o}_{1..t-1}$ are the control and observation history [62]. SLAM algorithms have been developed across sensing modalities, including LiDAR and RGB-D, with visual SLAM offering solutions based on feature matching [63], direct photometric tracking [64, 65], and visual-inertial fusion [66]. With growing efficiency and robustness, these methods output semidense 3D keypoints and time-aligned camera poses, providing structurally faithful and computationally efficient information about 3D scenes that users perceive and interact with from an egocentric perspective.

3.2 Keypoint Selection and Classification

Observation-based Keypoint Selection. An overview of EgoSpanLift is illustrated in Fig. 2. Our method initiates with a set of 3D semidense keypoints \mathcal{P} and localization information \mathcal{E} , typically obtained through visual SLAM [67]. Specifically, each $p_i \in \mathcal{P}$ consists of $(\mathbf{p}_i, \sigma_i, t_i)$, where $\mathbf{p}_i \in \mathbb{R}^3$

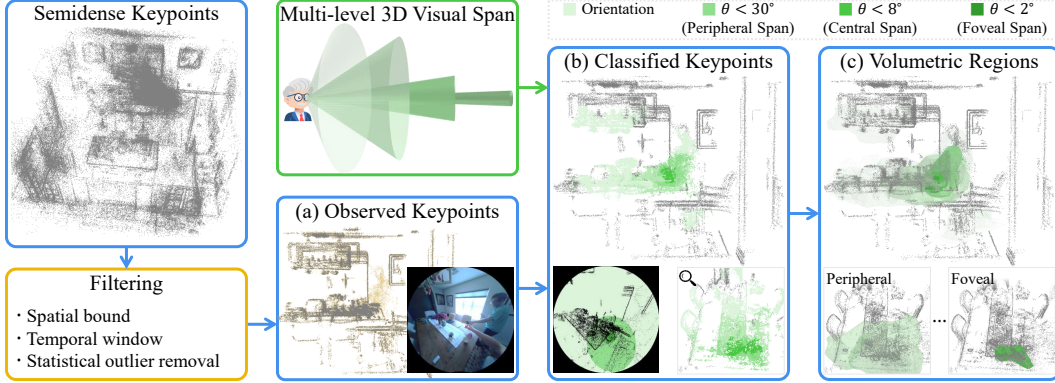


Figure 2: Overview of EgoSpanLift. Using 3D semidense keypoints from egocentric observations, e.g., SLAM, we filter observed keypoints at a given time window and leverage multi-level human visual span to compute volumetric regions in 3D scenes.

is the 3D keypoint in global coordinates, σ_i represents the confidence of estimation in the form of the variance of inverse distance, and t_i denotes the time at which the point was observed. Additionally, $\mathbf{E}_t \in \mathcal{E}$ represents an SE(3) element that transforms from the local egocentric frame (i.e., central pupil frame) at time t to the global coordinate system, i.e., $\mathbf{E}_t = \begin{pmatrix} \mathbf{R}_t & \mathbf{t}_t \\ \mathbf{0}^T & 1 \end{pmatrix}$, where the z -axis in the local coordinates denotes forward. From this, we obtain the set of keypoints observed at time t :

$$\mathcal{P}_t = \{p_i \in \mathcal{P} \mid t_i = t, \|\mathbf{p}_i - \mathbf{t}_t\|_1 < D/2, \mathcal{I}_f(p_i; \mathcal{P}_t) = 1\}, \quad (1)$$

where the first term serves as a filter that preserves visually observed keypoints at the given time, and the second term acts as a spatial filter that retains only points within a cubic boundary of length D around the user. The last term, $\mathcal{I}_f(p_i; \mathcal{P})$, is an indicator function returning the result of neighbor-based statistical outlier filtering f , where 1 indicates validity and 0 indicates invalidity.

We can establish the rationale for each filtering term as follows. For temporal filtering, we consider only a limited context within a temporal window spanning a few seconds before the current time rather than all keypoints observed from beginning to end. This enables operation without requiring an offline algorithm and prevents the inclusion of points that were visible from different viewpoints but are currently occluded (e.g., items inside the fridge). For spatial filtering, we restrict the area to prevent gaze from erroneously overshooting to distant locations and to focus on regions within the user’s vicinity that will be effectively perceived and interacted with. In most experiments, we used $D = 3.2\text{m}$, though we discuss experiments extending beyond 6m in Sec. 5.2. For outlier removal, we use neighbor-based statistical filtering instead of confidence-based filtering, i.e., σ_i , which is typically used when extracting static 3D scenes from SLAM outputs. This approach can retain important dynamic elements in egocentric scenes, such as moving people, the user’s hands, and other dynamic objects in the space, while effectively removing invalid points.

Gaze-based Keypoint Classification. Using keypoints from \mathcal{P}_t , we classify points that fall within a visual span defined around the user’s gaze direction after transforming each point to the local coordinates as $\mathbf{E}_t^{-1}\mathbf{p}_i$. To determine whether points are included in the visual span, we utilize a 3D gaze representation defined as a cone extending from the user. While some previous works have employed egocentric 3D representations in the form of directions or cones, e.g., intersection between gaze vectors and triangulated meshes of static objects [68] or overlap of multiple users’ gaze cones [69], our approach features a key distinction as it covers more general use cases by addressing which local regions of a 3D scene capture an *individual* user’s visual attention during daily activities without discriminating between *dynamic* and static components.

When the aforementioned gaze cone and keypoints at the local coordinates are projected onto the $z = 1$ plane, they are represented as green ellipses and black dots in the lower left of Fig. 2-(b). We select the dots that fall within these ellipses using the angular distance threshold θ (i.e., eccentricity):

$$Q_t^{\theta, \mathbf{g}_t} = \left\{ p_i \in \mathcal{P}_t \mid \frac{\langle \mathbf{E}_t^{-1}\mathbf{p}_i, \mathbf{g}_t \rangle}{\|\mathbf{E}_t^{-1}\mathbf{p}_i\| \|\mathbf{g}_t\|} > \cos \theta \right\}, \quad (2)$$

where $\langle \cdot, \cdot \rangle$ denotes inner product, and \mathbf{g}_t denotes the gaze direction in a local frame at time t . Through this, we can classify a set of points that correspond to the egocentric 3D visual span.

While employing SLAM for visual spans may pose challenges in modeling regions between semidense keypoints, our approach remains effective for two main reasons. First, human visual span or peripheral vision is known to be significantly influenced by contrast as well as eccentricity from the gaze direction [70, 71]. Since people overwhelmingly interact with visually salient objects rather than empty white walls, this approach is highly compatible with keypoints obtained through SLAM. Indeed, >99% of the 3D visual spans in our curated data samples from raw egocentric multisensory observations overlapped with SLAM keypoints. Furthermore, rather than relying on keypoints as inputs or outputs, we represent visual spans as volumetric regions derived from them, *e.g.*, Eq. 3, which provides good coverage of the given 3D scene and helps mitigate the aforementioned challenges.

3.3 Multi-level Volumetric Region Localization

Using classified keypoints $Q_t^{\theta, \mathbf{g}_t}$ in a cube of length D , we obtain regions corresponding to visual spans by computing their occupancy in a 3D Cartesian grid with resolution R and duration $[t_b, t_e]$:

$$V_{[t_b, t_e]}^{\theta, \mathbf{g}_t}(i, j, k) = \mathcal{I}(\{p_i \in \cup_{t \in [t_b, t_e]} Q_t^{\theta, \mathbf{g}_t} | \mathbf{0} \leq (p_i - \mathbf{t}_{t_b} + D/2) \times R/D - (i, j, k) \leq \mathbf{1}\} > 0), \quad (3)$$

where \mathcal{I} is an indicator function and $|\cdot|$ represents the cardinality of a set. This approach indirectly covers the regions not captured by semidense keypoints while maintaining constant space complexity regardless of the increasing number of points with longer durations. Also, since V is represented as a binary occupancy grid, computing the similarity between overlapped visual spans can be trivial.

Inspired by taxonomy defined in vision science literature [15], we categorize 3D volumetric regions of vision spans into four levels, as illustrated in Fig. 2. First, foveal localization $V^{\theta_f, \mathbf{g}_t}$ corresponds to the conventional 2D gaze localization area, covering a highly localized region with an eccentricity of $\theta_f = 2^\circ$. While foveal span exists in most regions, *i.e.*, around 80% in our curated dataset, there may be instances where it is absent due to our use of semidense keypoints. To address this limitation, we utilize spans corresponding to wider eccentricities: the central span $V^{\theta_c, \mathbf{g}_t}$ with $\theta_c = 8^\circ$ and the near peripheral span $V^{\theta_p, \mathbf{g}_t}$ with $\theta_p = 30^\circ$. Finally, regions observed in spans defined beyond these are significantly influenced by head orientation as much as the gaze, with a complex interplay between the two [72, 73]. Therefore, we employ the most broadly defined span as the region within the field-of-view centered on head orientation, *i.e.*, $V^{\theta_o, \mathbf{z}}$, which is analogous to the view frustum capturing visual input in 2D setups (*e.g.*, $\theta_o = 55^\circ$ in our experiments). Note that while continuous distributions such as Gaussian could be used, we analyze through the lens of this well-established taxonomy for intuitive evaluation and level-by-level integration across multiple timesteps.

As a result, for a given temporal window, we obtain multi-level volumetric regions that represent varying degrees of user visual attention focus in the surrounding environment. Since EgoSpanLift does not rely on time-consuming algorithms, when combined with existing platforms capable of real-time SLAM and gaze processing [74, 75, 76], it enables the acquisition of 3D information about human visual attention with trivial latency. Additionally, its representation as points or volumetric regions in a 3D Cartesian grid facilitates adaptation to existing 3D frameworks.

4 Forecasting Network

One of the most representative problems when considering a user’s visual span in 3D involves predicting future visual attention based on past contextual focus patterns. To this end, we introduce a straightforward framework to forecast 3D visual spans for future T_f frames, given the history of observations from past T_p frames, as illustrated in Fig. 3-(a). Note that our primary interest lies not in precisely matching what was seen in each respective frame but rather in understanding the trends and coverage areas of the user’s attention over a given period. To perform precise evaluation while minimizing the effects of exploration order of gaze, we use the union of visual spans over T_f frames as our prediction target.

Autoregressive Encoder. Given localization information $\mathcal{E}_{\text{prev}}$ and observed semidense keypoints $\mathcal{P}_{\text{prev}}$ for the past T_p seconds, we obtain multi-level volumetric regions representing previous visual spans through EgoSpanLift as described in Sec. 3. Specifically, we utilize a grid of size $T_p \times (4 + 1) \times R \times R \times R$ as input, where 4 represents visual spans ranging from orientation to foveal span,

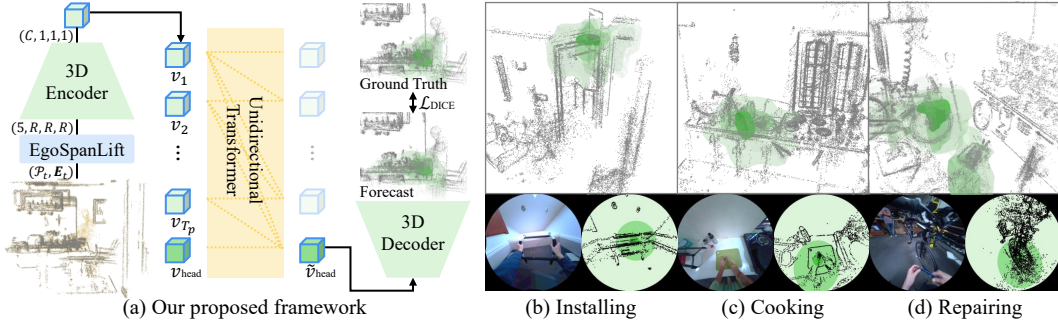


Figure 3: (a) Illustration of our framework and (b-d) diverse scenario examples in our curated dataset.

and 1 represents the complete scene in the given space regardless of span inclusion. To extract spatial features from this input grid, we initially compress them using the encoder of a 3D U-Net [77]. By reducing the spatial dimension by a factor of R through pooling, we obtain encoded features of size $T_p \times C$, where C is the feature dimension. Note that performing spatial reduction by a factor smaller than R showed negligible impact on performance.

While using T_p embeddings encodes how visual span has evolved over time, we separately incorporate a global embedding to serve as a prediction head. Thus, we utilize an embedding that encodes all visual spans within the duration as a global embedding, serving as our prediction head. By appending this embedding after the other embeddings, we obtain features of size $(T_p + 1) \times C$, *i.e.*, $v_1, \dots, v_{T_p}, v_{\text{head}}$. To learn temporal dependencies among these features and increase the model’s expressiveness, we employ a transformer with a unidirectional attention mask [78, 79], ensuring that information about temporal dynamics is integrated toward the final global embedding.

Decoder. Using the output embedding \tilde{v}_{head} that corresponds to v_{head} from the transformer, we perform upsampling via a U-Net decoder. During this process, we utilize intermediary features from the U-Net encoder through residual connections. By applying sigmoid, we ultimately obtain an output \tilde{Y}_{ijk} of size $4 \times R \times R \times R$ representing a 0-1 soft occupancy, which corresponds to our aggregated forecast of the user’s visual span over the future T_f frames.

Learning Objective. Since visual spans occupy only a very narrow region of the space surrounding the user, learning meaningful signals through conventional cross-entropy losses could be challenging. For instance, in the case of foveal span, almost all samples occupy less than 1% of the entire grid region. Therefore, we train our model using the dice loss with the ground truth forecast Y_{ijk} , where \odot is elementwise product:

$$\mathcal{L} = 1 - \frac{2 \times \sum \tilde{Y}_{ijk} \odot Y_{ijk}}{\sum \tilde{Y}_{ijk} + \sum Y_{ijk} + 1}. \quad (4)$$

Latency Analysis. Our framework has two primary sources of latency: (i) extracting the relevant set of points from gaze and SLAM keypoints (performed every 100ms), and (ii) performing model inference every second on a set of points spanning two seconds. Since the point extraction can be pre-computed and stored at 10 fps for continuous use, we only need to consider the computation time for processing the final observation when calculating inference latency. We measured this in a resource-constrained environment compared to our training setup, using 8 CPU cores and a GPU with 12GB VRAM.

Table 1: Latency analysis of our framework.

Operation	Latency
Point preprocessing	4.541±1.999ms
3D visual span localization	1.811±0.824ms
Voxelization	45.406±26.223ms
Model inference	19.483±8.234ms
Average latency	71.241ms

The results are summarized in Table 1. The first stage, which handles outlier removal, axis-aligned bounding box cropping for keypoints, and selection of points within a certain degree of eccentricity from the gaze, can be processed within 10ms. In the second stage, we identified that the primary bottleneck lies in voxelization rather than in the model itself. This occurs because the large number of keypoints from the previous stage should be voxelized, whereas the model operates efficiently once it receives the 3D voxelized representation. Consequently, the average inference latency is 71.241ms, yielding a real-time factor of 0.036, confirming our claim on fast processing capability. However, actual AR/VR environments typically operate with even fewer computational resources, and thus

Table 2: Comparison of forecasting accuracy on the FoVS-Aria test split. Higher the better.

Methods	Orientation		Peripheral _{30°}		Central _{8°}		Foveal _{2°}	
	IoU	F1	IoU	F1	IoU	F1	IoU	F1
2D Center Prior + EgoSpanLift + [80]	-	-	0.4061	0.5583	0.1621	0.2497	0.0685	0.1049
GLC [45] + EgoSpanLift + [80]	-	-	0.4553	0.6064	0.2227	0.3267	0.1321	0.1873
CSTS [20] + EgoSpanLift + [80]	-	-	0.4567	0.6076	0.2342	0.3423	0.1388	0.1948
OccFormer [81]	0.1395	0.2352	0.1106	0.1846	0.0429	0.0632	0.0158	0.0289
VoxFormer [82]	0.2192	0.3093	0.1847	0.2580	0.0915	0.1279	0.0453	0.0704
IAG [8]	0.3250	0.3669	0.2154	0.2542	0.1250	0.1851	0.0747	0.1050
EgoChoir [9]	0.4959	0.6579	0.4302	0.5581	0.2612	0.3608	0.1987	0.2311
Global Prior	0.1359	0.2314	0.1048	0.1825	0.0331	0.0618	0.0146	0.0280
Ours (w/o previous span)	0.3424	0.4906	0.2616	0.3928	0.1071	0.1739	0.0594	0.0828
Ours (\mathcal{L}_{BCE})	0.5730	0.7134	0.4594	0.6017	0.2836	0.3879	0.2059	0.2609
Ours (Gaze-only + [80])	-	-	<u>0.4723</u>	<u>0.6214</u>	0.2666	0.3791	0.2494	0.3193
Ours (Single-task)	<u>0.5832</u>	<u>0.7238</u>	0.4721	0.6154	<u>0.3351</u>	<u>0.4485</u>	0.2494	0.3193
Ours (w/o global embedding)	0.5602	0.7042	0.4647	0.6128	0.3241	0.4476	<u>0.2624</u>	<u>0.3487</u>
Ours (full)	0.5838	0.7247	0.4886	0.6350	0.3513	0.4762	0.2836	0.3709

additional optimization techniques such as model quantization or more efficient voxelization could be considered for further performance improvements.

5 Benchmarking Egocentric 3D Visual Span Forecasting

5.1 Forecasting Egocentric Daily Activities

Curation of FoVS-Aria. Due to the lack of an existing testbed for egocentric 3D visual span forecasting, we curate a dataset by processing the raw data streams from an existing egocentric multisensory dataset. Aria Everyday Activities dataset [23] encompasses diverse scenarios of people engaging in daily activities across different environments and interacting with others, comprising 143 recordings with a total duration of 7.3 hours. Initially, we inspect the SLAM keypoints and gaze scenarios of all recordings, manually filtering out cases with insufficient keypoints or those limited to stationary viewing of phones/TVs. Following recent research in 2D gaze anticipation [20], we define a sample as a 2-second prediction task based on a 2-second previous observation with a sliding window of 1 second. For spatial parameters, we use resolution $R = 16$ and cube length $D = 3.2m$, indicating that accurately matching a cell corresponds to precision within a $D/R = 20cm$ error margin. We construct the test split using all recordings from location 4 to enable the evaluation of unseen locations and the validation split by randomly stratifying the rest. Consequently, our constructed FoVS(Forecasting 3D Visual Span)-Aria consists of 23.2k samples in total, with 19.3k, 1.9k, and 2.1k samples for train, validation, and test splits, respectively.

Evaluation Protocol. For multi-level 3D visual span, we evaluate each level separately. We primarily utilize 3D IoU as a primary metric since our main concern is the overlap of volumetric regions. Additionally, we report F1 scores, commonly used in 2D gaze evaluation [45, 20], while precision and recall are reported in the Appendix. Finally, since the foveal span is defined within a highly narrow region, overlap-based metrics cannot fully capture its distribution. Therefore, we also examine the distribution of the (metric) distance between the ground truth region and the predicted region. Analysis on saliency-based metrics is deferred to Appendix.

Regarding baselines, due to lack of well-established frameworks for our task configuration, we construct applicable models from various domains. First, we adapt 3D localization methods like OccFormer [81] and VoxFormer [82] to predict visual span, which are known for effectively inferring semantic labels for voxels in outdoor driving scenarios. We also employ IAG [8] and EgoChoir [9], models designed to predict affordances or interaction hotspots in 3D from an egocentric user-object interaction perspective. Another framework includes state-of-the-art methods for 2D gaze anticipation, such as GLC [45] and CSTS [20]. Thanks to our EgoSpanLift, we can project these models' 2D inference results to 3D, extrapolating head pose information from past context using a multi-task Gaussian process model [80].

Comparison with Prior Arts. Table 2 presents comparative results among various methods. Overall, there is a substantial performance gap between existing methods and our approach, with the disparity becoming more pronounced when predicting more localized regions in 3D (*e.g.*, foveal span), where our method outperforms others by more than 50%. EgoChoir [9] displays the most promising performance among baselines, due to its capability of predicting 3D interaction hotspots that could be in line with user intentions. Compared to the other 3D localization methods, frameworks that consider the gaze dynamics show improved performance, despite falling significantly short on foveal span forecasting. This performance gap is further evidenced in Table 3, where baseline frameworks produce errors approximately twice as high as our approach on average.

Table 3: Distribution of metric errors in 3D foveal span localization.

Distance (cm)	min.	avg.	max.
GLC [45]	59.65	73.47	87.20
CSTS [20]	59.71	73.79	87.68
w/o prev. span	66.94	83.07	98.98
Single-task	36.54	52.90	69.18
Ours	19.04	34.85	51.23

Ablation Studies. The last six rows in Table 2 display the results of ablation studies on our methodology. The global prior—predicting answers based on the forecast distribution of the train split—yields considerably low numbers, implying that our FoVS-Aria encompasses diverse visual spans driven by various user intentions. Additionally, our model’s performance significantly deteriorates when attempting prediction without previous span information; this indicates that knowledge of where the user previously focused is crucial for accurate forecasting, as visual span can vary substantially according to intention. Using binary cross-entropy (BCE) as a loss function results in marginal performance degradation up to the central span level, but shows marked decline in foveal span performance. Similarly, jointly solving multi-level spans consistently outperforms the single-task approach, particularly benefiting foveal span improvement.

Multi-level interpretation carries significant implications due to uncertainties in self-motion forecasting and geometric correspondence between 2D and 3D spaces, as exemplified in suboptimal performance of predicting only gaze in 2D or 3D and applying postprocessing [80]. Two key conceptual differences between our framework and the postprocessing variant are (i) learning from multi-level representation and (ii) mitigating uncertainties in self-motion anticipation through end-to-end prediction. Leveraging the interconnection between gaze and periphery [15] allows us to capture cues about future gaze from previous periphery and forecast future periphery in light of previous gaze, which can be observed in several qualitative examples. Moreover, given the nature of the viewing frustum, extending 3D gaze predictions to broader spans necessitates the forecasting of ego-centric 6DoF pose trajectories with a separate postprocessing stage, which propagates uncertainties in self-motion forecasting and geometric correspondence between 2D and 3D spaces. In contrast, our end-to-end framework does not assume a specific forecast trajectory and predicts plausible 3D spans within the scene while implicitly learning to mitigate such uncertainties.

5.2 Forecasting Skilled Activities at Scale

Curation of FoVS-EgoExo. To analyze the effectiveness of visual span forecasting in skilled activities at a larger scale, we utilize Ego-Exo4D [24] as our source data, comprising hundreds of hours of observations. Ego-Exo4D consists of eight activity categories, from which we excluded soccer, basketball, and dance, as these activities involve overly large or dynamic scenes where clear fixations in visual spans are unidentifiable in the majority of cases. Instead, we focus on five categories: cooking, music, health, repair, and bouldering. After collecting only the footage corresponding to actual task execution, we refine the data and calculate volumetric regions following the same procedure used for FoVS-Aria. Considering the increased scale and the focus on specific tasks, we establish a 4-second prediction as the default setting. Thus, we collect a total of 341.4k samples, divided into 274.7k, 29.6k, and 37.0k samples for train, validation, and test splits, respectively.

Performance Analysis. Table 4 compares baseline model performance on FoVS-EgoExo. While our approach shows substantial performance gains over FoVS-Aria, presumably due to the nature of skilled activities and an order of magnitude larger sample size, the corresponding improvements in baseline methods are relatively modest. Unlike FoVS-Aria, the change of numbers regarding the orientation span likely stems from the inherent characteristics of skilled activities in FoVS-EgoExo, where participants tend to maintain more sustained focus on specific tasks rather than engaging in frequent, diverse head movements. Given that visual span forecasting prioritizes accurate prediction

Table 4: Comparison of forecasting accuracy on the FoVS-EgoExo test split. Higher the better.

Methods	Orientation		Peripheral _{30°}		Central _{8°}		Foveal _{2°}	
	IoU	F1	IoU	F1	IoU	F1	IoU	F1
CSTS [20] + EgoSpanLift + [80]	-	-	0.4978	0.6398	0.2867	0.4010	0.1556	0.2107
OccFormer [81]	0.1287	0.2280	0.0920	0.1685	0.0251	0.0490	0.0084	0.0167
VoxFormer [82]	0.1896	0.3188	0.1475	0.2571	0.0620	0.1168	0.0179	0.0350
EgoChoir [9]	0.3287	0.4948	0.2851	0.4437	0.1976	0.3300	0.1266	0.2247
Global Prior	0.2329	0.3621	0.2478	0.3776	0.1245	0.2119	0.0658	0.1188
Ours (w/o prev. span)	0.4091	0.5665	0.3876	0.5296	0.2855	0.4107	0.2255	0.3152
Ours (\mathcal{L}_{BCE})	0.5112	0.6621	0.4905	0.6338	0.3722	0.4867	0.2870	0.3578
Ours (w/o global embedding)	0.4998	0.6542	0.4892	0.6381	0.3954	0.5294	0.3475	0.4500
Ours (full)	0.5230	0.6743	0.5108	0.6569	0.4212	0.5541	0.3692	0.4702
$D = 3.2, R = 32$ (10cm)	0.4443	0.6040	0.4362	0.5893	0.3319	0.4656	0.2493	0.3497
$D = 6.4, R = 32$ (20cm)	0.4920	0.6462	0.4902	0.6394	0.4121	0.5464	0.3640	0.4689
$D = 3.2, R = 16$ (20cm)	0.5230	0.6743	0.5108	0.6569	0.4212	0.5541	0.3692	0.4702

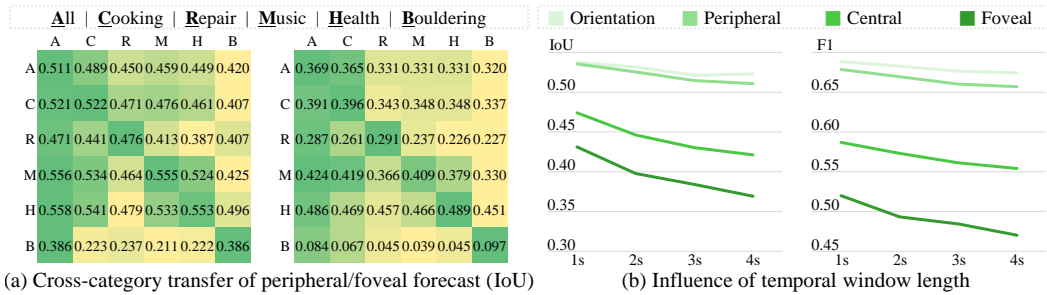


Figure 4: Analysis of our proposed framework on the FoVS-EgoExo test split.

of narrower regions, it is particularly noteworthy that substantial performance gaps exist between our method and baselines for Central and Foveal areas. These results indicate that skilled activity forecasting in FoVS-EgoExo is not inherently easier than daily activity forecasting in FoVS-Aria, while demonstrating that our model achieves robust performance across multiple scales and domains compared to prior arts.

We further analyze the impact of scale, category-specific training, and spatio-temporal granularity. According to experiments conducted with varying spatial configurations in Table 4, the impact on performance is marginal if the grid range is proportionally increased to maintain the same precision of 20cm despite an increased resolution of $R = 32$. However, for our model trained at 10cm precision with $R = 32$, performance decreases to levels similar to those observed in FoVS-Aria. Similarly, as demonstrated in Fig. 4-(b), performance tends to decline as we attempt to cover visual span further into the future, which is particularly significant when predicting foveal span.

Finally, cross-category transfer results are summarized in Fig. 4-(a). Despite significant variations in patterns across task categories, training an integrated model at sufficient scale achieves virtually identical performance to maintaining separate models for each category. Transfer among static tasks (e.g., cooking, music, and health) is relatively effective, but less so for more dynamic tasks such as repair or bouldering. Additionally, peripheral span, which covers wider areas or visual exploration, preserves performance better in cross-category scenarios compared to foveal span, which targets more localized regions. Qualitative examples can be found in Fig. 5-(b) and the Appendix.

5.3 Extension to 2D Gaze Anticipation

For completeness in our experimental analysis, we explore whether the reverse direction—from 3D to 2D—is also possible using our framework, given that we successfully extended egocentric visual span from 2D to 3D. To this end, we utilize samples from FoVS-Aria to compare 2D gaze anticipation performance. While our previous experiments in Table 2 required separate procedures like EgoSpanLift to bring 2D gaze models into 3D, deflating our model’s inference results to 2D can be accomplished trivially. We select the cell with maximum logit value from our model’s foveal span prediction and project it onto the 2D image plane using the user’s current head pose. Through

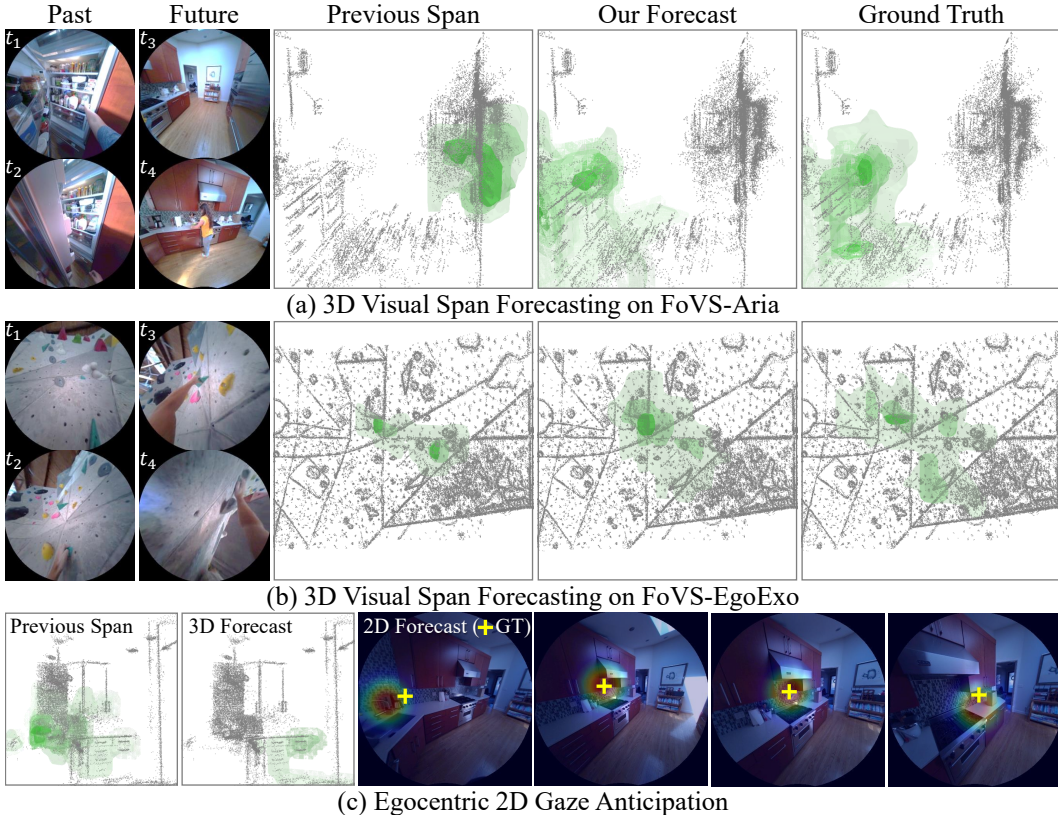


Figure 5: Qualitative examples. Our framework effectively forecasts various scenarios, such as (a) closing the fridge and turning around or (b) deciding which rocks to grab and navigate.

interpolation between the user’s current and projected gaze, we can easily obtain gaze anticipation results for the future two seconds.

The performance comparison results can be found in Table 5. Interestingly, while 2D methodologies struggled to accurately predict foveal span when transferred to 3D, our approach achieves on-par performance to models trained specifically for 2D despite not conducting any 2D-specific training. The baseline performance we obtained is slightly lower than that in the referenced paper [20], which we attribute to our exclusion of trivial recordings from FoVS-Aria like watching TV or smartphones.

Table 5: Comparison of egocentric 2D gaze anticipation.

	F1	Pr	Re
GLC [45]	0.505	0.453	0.571
CSTS [20]	0.515	0.497	0.535
Ours (Single)	0.505	0.432	0.608
Ours	0.515	0.440	0.619

6 Conclusion

We addressed the challenge of egocentric 3D visual span forecasting by designing a method that lifts multi-level visual span from 2D to 3D semidense keypoints and introducing an end-to-end framework for forecasting volumetric regions corresponding to each visual span. Furthermore, we curated a testbed for this problem by processing two datasets with raw multisensory observations, where we consistently outperformed a wide range of prior arts across all metrics. We anticipate that this framework will play a crucial role in proactively understanding human intent captured through perception that precedes interaction, enabling preemptive delivery of various latency-sensitive services. Future extensions of this work could incorporate forecasting problems for non-visual perception, such as auditory or proprioceptive inputs, or focus on forecasting highly precise attention tracking on dense scenes, which would represent particularly intriguing directions for further research.

Acknowledgment. This work was supported by Samsung Advanced Institute of Technology, Institute of Information & communications Technology Planning & Evaluation (IITP) grant funded by the Korea government (MSIT) (No. RS-2021-II211343, No. RS-2022-II220156, No. RS-2025-25442338), and National Research Foundation of Korea(NRF) funded by the Ministry of Education(RS-2023-00274280). This research was conducted as part of the Sovereign AI Foundation Model Project(Data Track), organized by the Ministry of Science and ICT(MSIT) and supported by the National Information Society Agency(NIA), S.Korea. Gunhee Kim is the corresponding author.

References

- [1] Dima Damen, Hazel Doughty, Giovanni Maria Farinella, Sanja Fidler, Antonino Furnari, Evangelos Kazakos, Davide Moltisanti, Jonathan Munro, Toby Perrett, Will Price, et al. Scaling egocentric vision: The epic-kitchens dataset. In *ECCV*, 2018.
- [2] Antonino Furnari and Giovanni Maria Farinella. What would you expect? anticipating egocentric actions with rolling-unrolling lstms and modality attention. In *ICCV*, 2019.
- [3] Yu Wu, Linchao Zhu, Xiaohan Wang, Yi Yang, and Fei Wu. Learning to anticipate egocentric actions by imagination. *IEEE TIP*, 2020.
- [4] Kristen Grauman, Andrew Westbury, Eugene Byrne, Zachary Chavis, Antonino Furnari, Rohit Girdhar, Jackson Hamburger, Hao Jiang, Miao Liu, Xingyu Liu, et al. Ego4d: Around the world in 3,000 hours of egocentric video. In *CVPR*, 2022.
- [5] Ye Yuan and Kris Kitani. Ego-pose estimation and forecasting as real-time pd control. In *ICCV*, 2019.
- [6] Wen Guo, Yuming Du, Xi Shen, Vincent Lepetit, Xavier Alameda-Pineda, and Francesc Moreno-Noguer. Back to mlp: A simple baseline for human motion prediction. In *WACV*, 2023.
- [7] Maria Escobar, Juanita Puentes, Cristhian Forigua, Jordi Pont-Tuset, Kevis-Kokitsi Maninis, and Pablo Arbelaez. Egocast: Forecasting egocentric human pose in the wild. In *WACV*, 2025.
- [8] Yuhang Yang, Wei Zhai, Hongchen Luo, Yang Cao, Jiebo Luo, and Zheng-Jun Zha. Grounding 3d object affordance from 2d interactions in images. In *ICCV*, 2023.
- [9] Yuhang Yang, Wei Zhai, Chengfeng Wang, Chengjun Yu, Yang Cao, and Zheng-Jun Zha. Egochoir: Capturing 3d human-object interaction regions from egocentric views. In *NeurIPS*, 2024.
- [10] Maurizio Corbetta and Gordon L Shulman. Control of goal-directed and stimulus-driven attention in the brain. *Nature Reviews Neuroscience*, 2002.
- [11] Samuel Tuhkanen, Jami Pekkanen, Paavo Rinkkala, Callum Mole, Richard M Wilkie, and Otto Lappi. Humans use predictive gaze strategies to target waypoints for steering. *Nature Scientific Reports*, 2019.
- [12] Soukayna Bekkali, George J Youssef, Peter H Donaldson, Jason He, Michael Do, Christian Hyde, Pamela Barhoun, and Peter G Enticott. Do gaze behaviours during action observation predict interpersonal motor resonance? *Social Cognitive and Affective Neuroscience*, 2022.
- [13] Charlie S Burlingham, Naveen Sendhilnathan, Oleg Komogortsev, T Scott Murdison, and Michael J Proulx. Motor “laziness” constrains fixation selection in real-world tasks. *PNAS*, 2024.
- [14] Keith Rayner. The perceptual span and peripheral cues in reading. *Cognitive Psychology*, 1975.
- [15] Hans Strasburger, Ingo Rentschler, and Martin Jüttner. Peripheral vision and pattern recognition: A review. *Journal of Vision*, 2011.
- [16] Pieter Bignaut. Visual span and other parameters for the generation of heatmaps. In *ETRA*, 2010.
- [17] Antje Nuthmann. On the visual span during object search in real-world scenes. *Visual Cognition*, 2013.
- [18] Freek Van Ede, Sammi R Chekroud, and Anna C Nobre. Human gaze tracks attentional focusing in memorized visual space. *Nature human behaviour*, 2019.
- [19] Mengmi Zhang, Keng Teck Ma, Joo Hwee Lim, Qi Zhao, and Jiashi Feng. Deep future gaze: Gaze anticipation on egocentric videos using adversarial networks. In *CVPR*, 2017.
- [20] Bolin Lai, Fiona Ryan, Wenqi Jia, Miao Liu, and James M Rehg. Listen to look into the future: Audio-visual egocentric gaze anticipation. In *ECCV*, 2024.

- [21] Anjul Patney, Marco Salvi, Jooheon Kim, Anton Kaplanyan, Chris Wyman, Nir Benty, David Luebke, and Aaron Lefohn. Towards foveated rendering for gaze-tracked virtual reality. *ACM TOG*, 2016.
- [22] Josef Spjut, Ben Boudaoud, Jonghyun Kim, Trey Greer, Rachel Albert, Michael Stengel, Kaan Akşit, and David Luebke. Toward standardized classification of foveated displays. *IEEE TVCG*, 2020.
- [23] Zhaoyang Lv, Nicholas Charron, Pierre Moulon, Alexander Gamino, Cheng Peng, Chris Sweeney, Edward Miller, Huixuan Tang, Jeff Meissner, Jing Dong, et al. Aria everyday activities dataset. *arXiv:2402.13349*, 2024.
- [24] Kristen Grauman, Andrew Westbury, Lorenzo Torresani, Kris Kitani, Jitendra Malik, Triantafyllos Afouras, Kumar Ashutosh, Vijay Baiyya, Siddhant Bansal, Bikram Boote, et al. Ego-exo4d: Understanding skilled human activity from first-and third-person perspectives. In *CVPR*, 2024.
- [25] Hyun Soo Park, Jyh-Jing Hwang, Yedong Niu, and Jianbo Shi. Egocentric future localization. In *CVPR*, 2016.
- [26] Heeseung Yun, Ruohan Gao, Ishwarya Ananthabhotla, Anurag Kumar, Jacob Donley, Chao Li, Gunhee Kim, Vamsi Krishna Ithapu, and Calvin Murdock. Spherical world-locking for audio-visual localization in egocentric videos. In *ECCV*, 2024.
- [27] Hao Jiang and Vamsi Krishna Ithapu. Egocentric pose estimation from human vision span. In *ICCV*, 2021.
- [28] Xucong Zhang, Yusuke Sugano, Mario Fritz, and Andreas Bulling. Appearance-based gaze estimation in the wild. In *CVPR*, 2015.
- [29] Kyle Krafka, Aditya Khosla, Petr Kellnhofer, Harini Kannan, Suchendra Bhandarkar, Wojciech Matusik, and Antonio Torralba. Eye tracking for everyone. In *CVPR*, 2016.
- [30] Yihua Cheng, Haofei Wang, Yiwei Bao, and Feng Lu. Appearance-based gaze estimation with deep learning: A review and benchmark. *IEEE TPAMI*, 2024.
- [31] Adria Recasens, Aditya Khosla, Carl Vondrick, and Antonio Torralba. Where are they looking? In *NIPS*, 2015.
- [32] Adria Recasens, Carl Vondrick, Aditya Khosla, and Antonio Torralba. Following gaze in video. In *ICCV*, 2017.
- [33] Danyang Tu, Xionghuo Min, Huiyu Duan, Guodong Guo, Guangtao Zhai, and Wei Shen. End-to-end human-gaze-target detection with transformers. In *CVPR*, 2022.
- [34] Benoît Massé, Silène Ba, and Radu Horaud. Tracking gaze and visual focus of attention of people involved in social interaction. *IEEE TPAMI*, 2017.
- [35] Yuchen Zhou, Linkai Liu, and Chao Gou. Learning from observer gaze: Zero-shot attention prediction oriented by human-object interaction recognition. In *CVPR*, 2024.
- [36] Yanyu Xu, Yanbing Dong, Junru Wu, Zhengzhong Sun, Zhiru Shi, Jingyi Yu, and Shenghua Gao. Gaze prediction in dynamic 360 immersive videos. In *CVPR*, 2018.
- [37] Julian Steil, Philipp Müller, Yusuke Sugano, and Andreas Bulling. Forecasting user attention during everyday mobile interactions using device-integrated and wearable sensors. In *MobileHCI*, 2018.
- [38] Zhiming Hu, Sheng Li, Congyi Zhang, Kangrui Yi, Guoping Wang, and Dinesh Manocha. Dgaze: Cnn-based gaze prediction in dynamic scenes. *IEEE TVCG*, 2020.
- [39] Zhiming Hu, Andreas Bulling, Sheng Li, and Guoping Wang. Fixationnet: Forecasting eye fixations in task-oriented virtual environments. *IEEE TVCG*, 2021.
- [40] Tim Rolff, H Matthias Harms, Frank Steinicke, and Simone Frintrop. Gazetransformer: Gaze forecasting for virtual reality using transformer networks. In *DAGM German Conference on Pattern Recognition*, 2022.
- [41] Sigrid Klerke, Yoav Goldberg, and Anders Søgaard. Improving sentence compression by learning to predict gaze. In *NAACL*, 2016.
- [42] Angela Lopez-Cardona, Carlos Segura, Alexandros Karatzoglou, Sergi Abadal, and Ioannis Arapakis. Seeing eye to ai: Human alignment via gaze-based response rewards for large language models. In *ICLR*, 2025.

- [43] Yifei Huang, Minjie Cai, Zhenqiang Li, and Yoichi Sato. Predicting gaze in egocentric video by learning task-dependent attention transition. In *ECCV*, 2018.
- [44] Yin Li, Miao Liu, and James M Rehg. In the eye of the beholder: Gaze and actions in first person video. *IEEE TPAMI*, 2021.
- [45] Bolin Lai, Miao Liu, Fiona Ryan, and James M Rehg. In the eye of transformer: Global-local correlation for egocentric gaze estimation. In *BMVC*, 2022.
- [46] Sven Bambach, Stefan Lee, David J Crandall, and Chen Yu. Lending a hand: Detecting hands and recognizing activities in complex egocentric interactions. In *ICCV*, 2015.
- [47] Guillermo Garcia-Hernando, Shanxin Yuan, Seungryul Baek, and Tae-Kyun Kim. First-person hand action benchmark with rgb-d videos and 3d hand pose annotations. In *CVPR*, 2018.
- [48] Fanqing Lin, Brian Price, and Tony Martinez. Ego2hands: A dataset for egocentric two-hand segmentation and detection. *arXiv:2011.07252*, 2020.
- [49] Minjie Cai, Feng Lu, and Yoichi Sato. Generalizing hand segmentation in egocentric videos with uncertainty-guided model adaptation. In *CVPR*, 2020.
- [50] Lingzhi Zhang, Shenghao Zhou, Simon Stent, and Jianbo Shi. Fine-grained egocentric hand-object segmentation: Dataset, model, and applications. In *ECCV*, 2022.
- [51] Bugra Tekin, Federica Bogo, and Marc Pollefeys. H+o: Unified egocentric recognition of 3d hand-object poses and interactions. In *CVPR*, 2019.
- [52] Taein Kwon, Bugra Tekin, Jan Stuhmer, Federica Bogo, and Marc Pollefeys. H2o: Two hands manipulating objects for first person interaction recognition. *arXiv:2104.11181*, 2021.
- [53] Takehiko Ohkawa, Kun He, Fadime Sener, Tomáš Hodaň, Luan Tran, and Cem Keskin. Assemblyhands: Towards egocentric activity understanding via 3d hand pose estimation. In *CVPR*, 2023.
- [54] Yana Hasson, Gul Varol, Dimitrios Tzionas, Igor Kalevatykh, Michael J Black, Ivan Laptev, and Cordelia Schmid. Learning joint reconstruction of hands and manipulated objects. In *CVPR*, 2019.
- [55] Yu-Wei Chao, Wei Yang, Yu Xiang, Pavlo Molchanov, Ankur Handa, Jonathan Tremblay, Yashraj S Narang, Karl Van Wyk, Umar Iqbal, Stan Birchfield, et al. Dexycb: A benchmark for capturing hand grasping of objects. In *CVPR*, 2021.
- [56] Yunze Liu, Yun Liu, Che Jiang, Kangbo Lyu, Weikang Wan, Hao Shen, Boqiang Liang, Zhoujie Fu, He Wang, and Li Yi. Hoi4d: A 4d egocentric dataset for category-level human-object interaction. In *CVPR*, 2022.
- [57] Ahmad Darkhalil, Dandan Shan, Bin Zhu, Jian Ma, Amlan Kar, Richard Higgins, Sanja Fidler, David Fouhey, and Dima Damen. Epic-kitchens visor benchmark: Video segmentations and object relations. *NeurIPS*, 2022.
- [58] Yiming Li, Ziang Cao, Andrew Liang, Benjamin Liang, Luoyao Chen, Hang Zhao, and Chen Feng. Egocentric prediction of action target in 3d. In *CVPR*, 2022.
- [59] Wentao Bao, Lele Chen, Libing Zeng, Zhong Li, Yi Xu, Junsong Yuan, and Yu Kong. Uncertainty-aware state space transformer for egocentric 3d hand trajectory forecasting. In *ICCV*, 2023.
- [60] Irving Fang, Yuzhong Chen, Yifan Wang, Jianghan Zhang, Qiushi Zhang, Jiali Xu, Xibo He, Weibo Gao, Hao Su, Yiming Li, et al. Egopat3dv2: Predicting 3d action target from 2d egocentric vision for human-robot interaction. In *ICRA*, 2024.
- [61] Kumar Ashutosh, Georgios Pavlakos, and Kristen Grauman. Fiction: 4d future interaction prediction from video. In *CVPR*, 2025.
- [62] Hugh Durrant-Whyte and Tim Bailey. Simultaneous localization and mapping: part i. *IEEE Robotics & Automation Magazine*, 2006.
- [63] Raul Mur-Artal, Jose Maria Martinez Montiel, and Juan D Tardos. Orb-slam: A versatile and accurate monocular slam system. *IEEE Transactions on Robotics*, 2015.
- [64] Jakob Engel, Thomas Schöps, and Daniel Cremers. Lsd-slam: Large-scale direct monocular slam. In *ECCV*, 2014.

- [65] Jakob Engel, Vladlen Koltun, and Daniel Cremers. Direct sparse odometry. *IEEE TPAMI*, 2017.
- [66] Tong Qin, Peiliang Li, and Shaojie Shen. Vins-mono: A robust and versatile monocular visual-inertial state estimator. *IEEE Transactions on Robotics*, 2018.
- [67] Jakob Engel, Kiran Somasundaram, Michael Goesele, Albert Sun, Alexander Gamino, Andrew Turner, Arjang Talattof, Arnie Yuan, Bilal Souti, Brighid Meredith, et al. Project aria: A new tool for egocentric multi-modal ai research. *arXiv:2308.13561*, 2023.
- [68] Dima Damen, Teesid Leelasawassuk, Osian Haines, Andrew Calway, and Walterio W Mayol-Cuevas. You-do, i-learn: Discovering task relevant objects and their modes of interaction from multi-user egocentric video. In *BMVC*, 2014.
- [69] Hyun Soo Park, Eakta Jain, and Yaser Sheikh. 3d social saliency from head-mounted cameras. *NIPS*, 2012.
- [70] Hans Strasburger, Lewis O Harvey, and Ingo Rentschler. Contrast thresholds for identification of numeric characters in direct and eccentric view. *Perception & psychophysics*, 1991.
- [71] Pia Mäkelä, Risto Näsänen, Jyrki Rovamo, and Dean Melmoth. Identification of facial images in peripheral vision. *Vision Research*, 2001.
- [72] Ryoichi Nakashima and Satoshi Shioiri. Why do we move our head to look at an object in our peripheral region? lateral viewing interferes with attentive search. *PLoS one*, 2014.
- [73] Yumiko Otsuka and Colin WG Clifford. Influence of head orientation on perceived gaze direction and eye-region information. *Journal of Vision*, 2018.
- [74] Andrew J Davison, Ian D Reid, Nicholas D Molton, and Olivier Stasse. Monoslam: Real-time single camera slam. *IEEE TPAMI*, 2007.
- [75] Tobias Fischer, Hyung Jin Chang, and Yiannis Demiris. Rt-gene: Real-time eye gaze estimation in natural environments. In *ECCV*, 2018.
- [76] Meta. Introducing Aria Gen 2: Unlocking New Research in Machine Perception, Contextual AI, Robotics, and More. <https://www.meta.com/blog/project-aria-gen-2-next-generation-egocentric-research-glasses-reality-labs-ai-robotics/>, 2025.
- [77] Özgün Çiçek, Ahmed Abdulkadir, Soeren S Lienkamp, Thomas Brox, and Olaf Ronneberger. 3d u-net: learning dense volumetric segmentation from sparse annotation. In *MICCAI*, 2016.
- [78] Ashish Vaswani, Noam Shazeer, Niki Parmar, Jakob Uszkoreit, Llion Jones, Aidan N Gomez, Łukasz Kaiser, and Illia Polosukhin. Attention is all you need. *NIPS*, 2017.
- [79] Alec Radford, Karthik Narasimhan, Tim Salimans, and Ilya Sutskever. Improving language understanding by generative pre-training. 2018.
- [80] Jacob Gardner, Geoff Pleiss, Kilian Q Weinberger, David Bindel, and Andrew G Wilson. Gpytorch: Blackbox matrix-matrix gaussian process inference with gpu acceleration. In *NeurIPS*, 2018.
- [81] Yunpeng Zhang, Zheng Zhu, and Dalong Du. Occformer: Dual-path transformer for vision-based 3d semantic occupancy prediction. In *ICCV*, 2023.
- [82] Yiming Li, Zhiding Yu, Christopher Choy, Chaowei Xiao, Jose M Alvarez, Sanja Fidler, Chen Feng, and Anima Anandkumar. Voxformer: Sparse voxel transformer for camera-based 3d semantic scene completion. In *CVPR*, 2023.
- [83] Qiao Gu, Zhaoyang Lv, Duncan Frost, Simon Green, Julian Straub, and Chris Sweeney. Egolifter: Open-world 3d segmentation for egocentric perception. In *ECCV*, 2024.